



The immunocytokine L19-IL2: An interplay between radiotherapy and long-lasting systemic anti-tumour immune responses

Nicolle H. Rekers ^{a,*}, Veronica Olivo Pimentel^{a,*}, Ala Yaromina^a, Natasja G. Lieuwes^a, Rianne Biemans^a, Catharina M. L. Zegers^a, Wilfred T. V. Germeraad^b, Evert J. Van Limbergen^a, Dario Neri^c, Ludwig J. Dubois ^{a,**}, and Philippe Lambin^{a,d,**}

^aDepartment of Radiotherapy, The M-Lab group, GROW - School for Oncology and Developmental Biology, Maastricht Comprehensive Cancer Centre, Maastricht University Medical Centre, Maastricht, The Netherlands; ^bDepartment of Internal Medicine, Division of Hematology, GROW - School for Oncology and Developmental Biology, Maastricht Comprehensive Cancer Centre, Maastricht University Medical Centre, Maastricht, The Netherlands; ^cDepartment of Chemistry and Applied Biosciences, Swiss Federal Institute of Technology, Zürich, Switzerland; ^dDepartment of Radiotherapy, The D-Lab, GROW - School for Oncology and Developmental Biology, Maastricht Comprehensive Cancer Center, Maastricht University Medical Center, Maastricht, The Netherlands

ABSTRACT

Recently, we have shown that the administration of the tumour-targeted antibody-based immunocytokine L19-IL2 after radiotherapy (RT) resulted in synergistic anti-tumour effect. Here we show that RT and L19-IL2 can activate a curative abscopal effect, with a long-lasting immunological memory. Ionizing radiation (single dose of 15Gy, 5 × 2Gy or 5 × 5Gy) was delivered to primary C51 colon tumour-bearing immunocompetent mice in combination with L19-IL2 and response of secondary non-irradiated C51 or CT26 colon tumours was evaluated. 15Gy + L19-IL2 triggered a curative (20%) abscopal effect, which was T cell dependent. Moreover, 10Gy + L19-IL2 treated and cured mice were re-injected after 150 days with C51 tumour cells and tumour uptake was assessed. Age-matched controls (matrigel injected mice treated with 10Gy + L19-IL2, mice cured after treatment with surgery + L19-IL2 and mice cured after high dose RT 40Gy + vehicle) were included. Several immunological parameters in blood, tumours, lymph nodes and spleens were investigated. Treatment with 10Gy + L19-IL2 resulted in long-lasting immunological memory, associated with CD44⁺CD127⁺ expression on circulating T cells. This combination treatment can induce long-lasting curative abscopal responses, and therefore it has also great potential for treatment of metastatic disease. Preclinical findings have led to the initiation of a phase I clinical trial (NCT02086721) in our institute investigating stereotactic ablative radiotherapy with L19-IL2 in patients with oligometastatic solid tumours.

ARTICLE HISTORY

Received 24 April 2017
Revised 30 November 2017
Accepted 2 December 2017

KEYWORDS

abscopal effect;
immunotherapy; memory
effect; L19-IL2; Radiotherapy;
tumour

Introduction

Radiotherapy (RT) is known to enhance the release of a broad range of tumour-associated antigens and damage associated molecular patterns (DAMPs). It also stimulates the upregulation of immunomodulatory cell surface molecules. Together, this results in a personified ‘*in situ* vaccine’ thereby initiating an immune response.¹⁻³ These changes in tumour immunogenicity promote the uptake of tumour antigens by dendritic cells that cross-present the tumour antigens to T cells, thereby triggering a cytotoxic T-lymphocyte response.^{1,3-5} In some cases, tumour regression outside the radiation field can be observed, a phenomenon known as the abscopal effect.⁶⁻¹¹ Its clinical appearance however is sporadic.¹² It has been established that the RT-induced abscopal effect is immune mediated¹³⁻¹⁸ and therefore the rationale of combining RT with immunotherapeutic approaches to further increase systemic anti-tumour effects has recently gained a lot of interest.¹⁹

The cytokine interleukin 2 (IL2) stimulates the proliferation and differentiation of cytotoxic, helper and regulatory T cells,

and natural killer (NK) cells, resulting in a balanced pro- and anti-inflammatory immune response.²⁰ IL2 treatment has shown durable and curative regressions in patients with metastatic melanoma, renal cancer and advanced non-Hodgkin’s lymphomas and represents the first effective immunotherapy.^{21,22} However, further clinical systemic use has been hampered due to the appearance of several severe toxicities (e.g. capillary leakage syndrome, severe flu-like symptoms, and coma).²³ Specific targeting of IL2 to the tumour using the vehicle L19, an antibody fragment directed against the angiogenesis-associated B-fibronectin isoform ectodomain-B (ED-B) typically overexpressed in solid tumours, resulted in high intra-tumoural IL2 concentrations without increasing toxicity.²⁴ The immunocytokine L19-IL2 has been investigated in a randomized phase II clinical trial in patients with metastatic melanoma in combination with dacarbazine or with L19-TNF α (tumour necrosis factor) showing encouraging anti-tumour activity.²⁵⁻²⁹ Furthermore, tumour-specific (neo)antigens are important recognition sites for

CONTACT Ludwig J. Dubois  ludwig.dubois@maastrichtuniversity.nl  Universiteitssingel 50/23, PO Box 616, 6200 MD Maastricht, The Netherlands.

 Supplemental data for this article can be accessed on the [publisher's website](#).

*Equal contribution.

**Equal contribution.

© 2018 Nicolle H. Rekers, Veronica Olivo Pimentel, Ala Yaromina, Natasja G. Lieuwes, Rianne Biemans, Catharina M. L. Zegers, Wilfred T. V. Germeraad, Evert J. Van Limbergen, Dario Neri, Ludwig J. Dubois and Philippe Lambin. Published with license by Taylor & Francis Group, LLC
This is an Open Access article distributed under the terms of the Creative Commons Attribution-NonCommercial License (<http://creativecommons.org/licenses/by-nc/4.0/>), which permits unrestricted non-commercial use, distribution, and reproduction in any medium, provided the original work is properly cited.

immune cells^{30–32} and since RT increases the tumour (neo)antigen expression it has great immunotherapeutic improving potential for all solid tumours.⁵

Recently, we have demonstrated that the combination of a single RT dose with L19-IL2 resulted in long-lasting, highly synergistic anti-tumour effects with a cure rate of 75% in the high ED-B expressing C51 mouse colon carcinoma. Expression of ED-B as well as infiltration of CD8⁺ T cells was crucial for this pronounced anti-tumour immune response.³³ Similar to the C51 tumour model, ED-B is overexpressed in the majority of solid tumours,^{34–38} making this combination therapy of great clinical interest. This highly synergistic preclinical finding resulted in the initiation of a phase I clinical study (NCT02086721) in our institute, in which stereotactic radiotherapy is combined with L19-IL2 in non-small cell lung cancer patients with oligometastatic tumours.

Our ultimate goal is to increase progression-free survival in patients with (oligo)metastatic cancer. However, high tumour burden and invisible (micro)metastases limit the applicability of radiotherapy in these patients. In the current study, we have investigated the systemic and long-lasting anti-tumour effects elicited by RT combined with L19-IL2, providing us insights into their synergistic interplay and induced immune responses. Since we have shown that the synergistic effect of RT + L19-IL2 against irradiated tumours is highly dependent on the immune system, we hypothesize that this combination therapy can elicit an abscopal effect targeting macroscopic tumours outside the radiation field. This study compares fractionated and single dose RT, irradiated and non-irradiated tumours, responding and non-responding mice and differences in potential to induce long-lasting protection (memory effect).

Results

A single RT dose combined with L19-IL2 triggers a curative abscopal effect

Previously we have demonstrated that single dose RT in combination with L19-IL2 provides an enhanced effect against primary C51 tumours.³³ In the present study, to test whether RT + L19-IL2 results in an abscopal effect, RT was locally delivered to one of the C51 tumours (primary) growing on contralateral flanks in combination with systemic L19-IL2 treatment. Single dose 15Gy or fractionated irradiation with 5 × 2Gy has been selected since pilot experiments demonstrated that these radiation doses combined with L19-IL2 result in 100% cure of primary tumours (supplementary Fig. 1). 5 × 5Gy + L19-IL2 was included in the abscopal experiments being the biologically equivalent to 15Gy (Fig. 1A and B). The distribution of volumes of secondary (non-irradiated) tumours at start of treatment was similar across different treatment groups (supplementary table 1). Secondary tumours of mice treated with 15Gy + L19-IL2 showed a significantly longer median T4xSV (9.6 [4.3–26.4] days) as compared to 15Gy + vehicle (5.7 [5.1–8.9] days, $p = 0.03$) with a cure rate of 20% (2/10) (Fig. 1B). Addition of L19-IL2 to 5 × 2Gy significantly increased T4xSV of the non-irradiated tumours from 5.9 [3.1–7.7] days to 8.8 [5.7–17.6] days ($p = 0.003$), to a similar extent as 5 × 5Gy + L19-IL2 (T4xSV of 10.1 [6.6–12.9] days). In contrast to 15Gy, none of the secondary tumours of the

fractionated RT groups could be cured (Fig. 1B). Tumour volumes over time in this abscopal experimental setup are shown in supplementary Fig. 2.

For a single 15Gy RT dose in combination with L19-IL2, we observed at day 4a significantly higher percent of CD4⁺ T cells inside secondary tumours (8.3% [2.9–42.3]) as compared with the primary tumours (2.0% [0.2–3.4], $p = 0.02$) (Fig. 1C). In addition, the percentage of CD4⁺ T cells in 15Gy + L19-IL2 treated tumours is significantly lower as compared with L19-IL2 treated tumours (4.1% [1.2–5.2], $p = 0.02$). At this time point, no differences in infiltrating CD8⁺ cytotoxic T cells could be observed (Fig. 1C).

The curative abscopal effect is dependent on T cells

To assess the causal relationship between the anti-tumour abscopal effect and T cells, we depleted CD4⁺ T or CD8⁺ T cells at day 5 after RT (Fig. 2A, supplementary table 1) using mice bearing C51 tumours. CD8⁺ and CD4⁺ T cells were successfully depleted 2 days after the first i.p. injection of depleting antibodies to 0.2% [0–0.6] and 0% as compared to IgG control: 9.2% [6.2–13.7, $p = 0.003$] and 36.0% [19.2–52.5, $p = 0.003$], respectively (Fig. 2A). Depletion of CD8⁺ or CD4⁺ T cells had little to no effect on the treatment response of irradiated primary tumours (supplementary Fig. 3A), suggesting that the immunological activity against these tumours has largely been completed and it is likely that the abscopal effect has already been initiated at the time point when depleting antibodies were administered. IgG treatment resulted in 29% (2/7) cure rate of secondary non-irradiated tumours (Fig. 2B) consistent with the results obtained in the previous independent experiment (Fig. 1B). Abscopal tumour response was not changed upon CD4⁺ T cell depletion as compared to IgG control ($p = 0.21$) (Fig. 2B). Depletion of CD8⁺ T cells resulted in significantly ($p = 0.01$) faster growth of secondary tumours as compared to IgG control, demonstrating a causal role for cytotoxic T cells in the RT + L19-IL2 induced abscopal effect. Volumes of non-irradiated tumours over time and tumour volumes at start of depletion are shown in supplementary Fig. 3B and C, respectively.

Next, we investigated the specificity of the abscopal effect, using the ED-B positive CT26 tumour³⁹ as a non-irradiated secondary tumour (Fig. 2C, supplementary table 1). In contrast to the matched C51 secondary tumours, which showed a significantly ($p = 0.026$) enhanced response to 15Gy + L19-IL2 as compared with 15Gy + vehicle, this effect was not observed ($p = 0.095$) in CT26 tumour (Fig. 2D). In addition, tumour response was not different between the secondary C51 and CT26 tumours for mice treated with 15Gy + L19-IL2, although no tumour cures could be observed in the latter group (Fig. 2D).

A single RT dose combats the intratumoural immunosuppressive T cell phenotype

We have shown that 15Gy + L19-IL2 induced a curative abscopal effect in only 20–30% of the non-irradiated tumours (Fig. 1B, Fig. 2B), depending on the experiment. We hypothesized that the same immune response triggered by this treatment combination is immunosuppressive in non-irradiated tumours. To test this, we investigated the expression of FoxP3 (an intracellular marker for regulatory T cells) and the

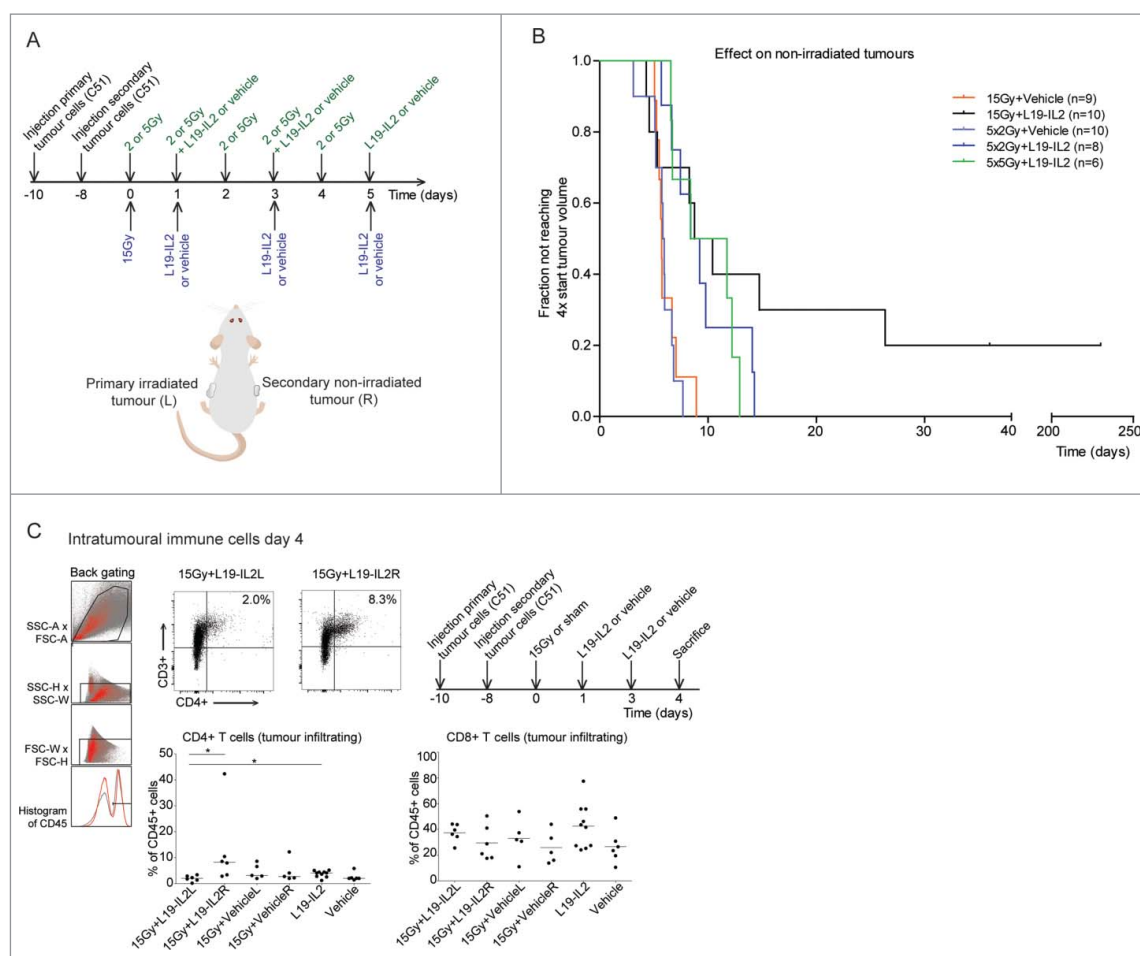


Figure 1. Radiotherapy and L19-IL2 induced abscopal effects and immune infiltration. (A) Experimental setup and schedule used for abscopal study. Each mouse was injected with tumour cells on the left flank on day -10 and on the right flank on day -8 . (B) The fraction of non-irradiated tumours not reaching 4 times start tumour volume. n = number of non-irradiated tumours (one per mouse). Treatment of mice with 15Gy + vehicle, 15Gy + L19-IL2, 5 \times 2Gy + vehicle and 5 \times 2Gy + L19-IL2 was performed in one single experiment (27 mice in total) and treatment with 5 \times 5Gy + L19-IL2 was performed in an additional experiment ($n = 6$). (C) Representative back gating (red), FACS image showing intratumoural CD3⁺CD4⁺ cells of gated CD45⁺ cells of irradiated (L) and non-irradiated (R) tumours, a quantification of the intratumoural CD3⁺CD4⁺ and CD3⁺CD8⁺ cells and the experimental schedule used. * $p < 0.05$. Bars represent median.

targetable immunosuppressive checkpoint receptors CTLA-4 and PD-1 on peripheral and intratumoural T cells.

Although non-irradiated tumours from mice treated with 15Gy + L19-IL2 did not show higher PD-1 (Fig. 3A) or CTLA-4 (data not shown) expression on CD8⁺ T cells as compared to irradiated tumours, significantly more CD4⁺ T cells expressed PD-1 (4.2% [1.7–6.7]) in non-irradiated secondary tumours than in irradiated primary tumours (0.8% [0.1–1.6], $p = 0.002$) and vehicle control (0.9% [0.8–5.0], $p = 0.02$) (Fig. 3B). Furthermore, the non-irradiated tumours showed a higher percent of CD25⁺FoxP3⁺CD4⁺ T cells (1.8% [0.4–6.6]) as compared with the irradiated tumours (0.2% [0.04–1.3], $p = 0.009$) (Fig. 3B). Strikingly, irradiated (15Gy) tumours after L19-IL2 showed a significantly lower percent of CD4⁺PD-1⁺ T cells (0.8%, [0.1–1.6]) in comparison with 15Gy + vehicle (2% [1.3–4.6], $p = 0.01$) and L19-IL2 only treated tumours (2.2% [0.5–3.0], $p = 0.005$). A significantly lower percentage of FoxP3⁺CD25⁺CD4⁺ T cells in irradiated tumours after RT + L19-IL2 (0.2% [0.04–1.3]) as compared with L19-IL2 monotherapy (1.7% [0.4–2.4], $p = 0.01$) was also observed. These data show that the addition of a single dose of 15Gy to the L19-IL2 monotherapy combats the immunosuppressive T cell

infiltrate in irradiated tumours. Interestingly, this immunosuppressive combating potential could not be observed when combining L19-IL2 with fractionated RT (5 \times 2Gy) (Fig. 3C). Although CD4⁺ and CD8⁺ T cell tumour infiltration was not significantly different between the irradiated and non-irradiated tumours (Fig. 3D, E), the addition of L19-IL2 to fractionated RT increased percent of CD8⁺PD-1⁺ infiltrating cells in non-irradiated tumours (20.1% [8.6–38.3]) as compared to 5 \times 2Gy + vehicle treated non-irradiated tumours (7.5% [4.0–8.9], $p = 0.01$) (Fig. 3D). Furthermore, addition of L19-IL2 to fractionated RT significantly increased percent of CD4⁺PD-1⁺ T cells in irradiated tumours (2% [1.2–2.7]) as compared to the vehicle treated primary tumours (0.9% [0.5–2], $p = 0.01$) (Fig. 3E).

No differences in peripheral CD4⁺ (data not shown) and CD8⁺ T cells were observed between all treatment groups (supplementary Fig. 4A). Interestingly, fractionated RT resulted in a higher percent of CD8⁺PD-1⁺ T cells when combined with L19-IL2 (13% [1.8–25.1]) as compared with 5 \times 2Gy + vehicle treated mice (1.2% [0.4–12.1], $p = 0.03$) (supplementary Fig. 4B). No differences were observed for CD4⁺PD-1⁺ T cells (data not shown).

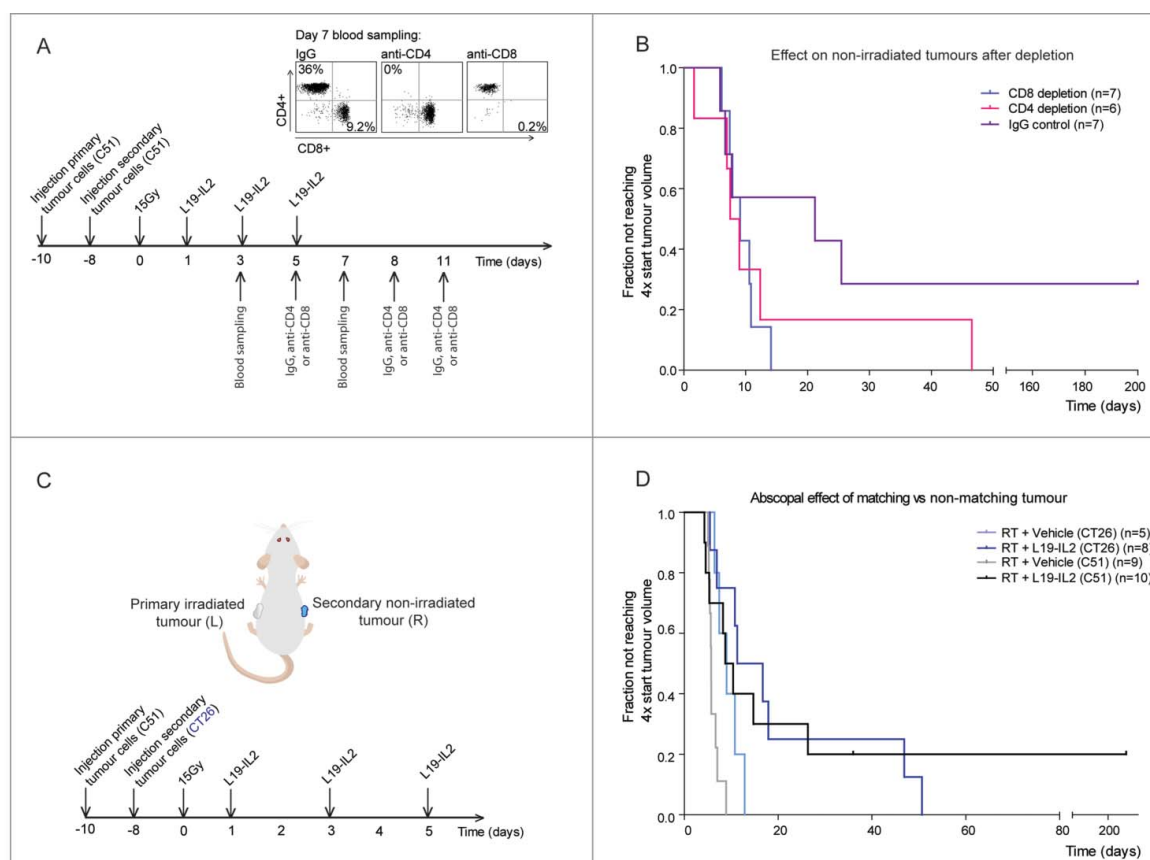


Figure 2. The abscopal effect in T cells depleted and mismatched tumour-bearing mice. Each mouse was injected with one tumour on the left flank on day -10 and with one tumour on the contralateral flank on day -8 . (A) Depletion study schedule and FACS to confirm depletion of CD4⁺ or CD8⁺ T cells in blood. (B) Fraction of tumours not reaching 4 times start tumour volume. n = number of non-irradiated tumours. This depletion study was performed once, using 20 mice in total. (C) Experimental setup and schedule used for abscopal study using mismatched (CT26) secondary tumours. (D) Fraction of tumours not reaching 4 times start tumour volume for the different treatment groups. n = number of non-irradiated tumours. For C51 (matched) tumours, we used the same groups as described in Fig. 1 to compare them with the mismatched tumours.

Immunological responses after single doses and fractionated irradiation

To explore the differences in the magnitude of abscopal effect induced by single dose and biologically equivalent fractionated RT + L19-IL2, we investigated mice at day 5 after start of treatment (Fig. 4A). Mice treated with $5 \times 5\text{Gy}$ + L19-IL2 had a significantly lower number of peripheral blood CD4⁺ T cells (8.7% [5.5–12.4] $p = 0.04$) as compared with 15Gy + L19-IL2 treated mice (19.6% [6.2–29.2]) (Fig. 4B). No differences in PD-1⁺, CTLA-4⁺ or FoxP3⁺CD25⁺ T cells were found (Fig. 4B) as well as percent of CD8⁺ T cells and sub-populations (data not shown). At this time point, no differences in total number of tumour infiltrating CD4⁺ T cells could be observed (data not shown). The percentage of infiltrating CD8⁺ T cells, however, was significantly higher in the 15Gy + L19-IL2 (49.3% [33.9–63]) as compared with $5 \times 5\text{Gy}$ + L19-IL2 (23.4% [3.7–48.8], $p = 0.03$). The expression of PD-1 and CTLA-4 on CD8⁺ T cells was not significantly different (Fig. 4C). Supplementary Fig. 5 shows the gating strategy used for the analyses.

Long-lasting immunological memory associated with CD44⁺CD127⁺CD8⁺ T cells

Next we investigated if the anti-tumour immune response modulated by RT + L19-IL2 remains active against its target,

i.e. the tumour-associated (neo)antigens. To test this hypothesis, mice cured from C51 tumours by a single dose of 10Gy + L19-IL2,³³ were re-injected with C51 tumour cells 150 days after injection. While age-matched naive mice reached a tumour volume of 500 mm³ within 17 days after cell injection, none of the cured mice showed tumour formation (Fig. 5A). Although not significant, FACS analyses at endpoint revealed a higher percent of CD8⁺ T cells co-expressing CD44⁺CD127⁺ in spleens (Fig. 5B) and lymph nodes (data not shown) in the re-challenged mice that were able to reject tumours (4.8% [0.9–6.4]) as compared with naive (0.9% [0.3–1.7]) and tumour-bearing (1% [0.8–1.8]) age-matched controls (Fig. 5B).

Next, we investigated whether this long-lasting anti-tumour response solely depends on tumour cure by RT + L19-IL2 treatment and on CD127 expressing T cells. For this, in an independent experiment, 150 days after tumor implantation, mice cured by either 10Gy + L19-IL2, surgery + L19-IL2 or high dose RT (40Gy) (supplementary Fig. 6A) were re-challenged with C51 tumours. In 10Gy + L19-IL2 treatment group either CD127 blocking antibody or IgG control antibody was applied. Three days after the start of CD127 blocking, the expression of CD127 on CD3⁺ cells was significantly ($p = 0.004$) lower as compared with the IgG treated (Fig. 5C). Eight out of 12 mice cured by 10Gy + L19-IL2, were not able to form new tumours and blocking of CD127 had no influence on this protective effect (Fig. 5D). Therefore, for further analyses, these

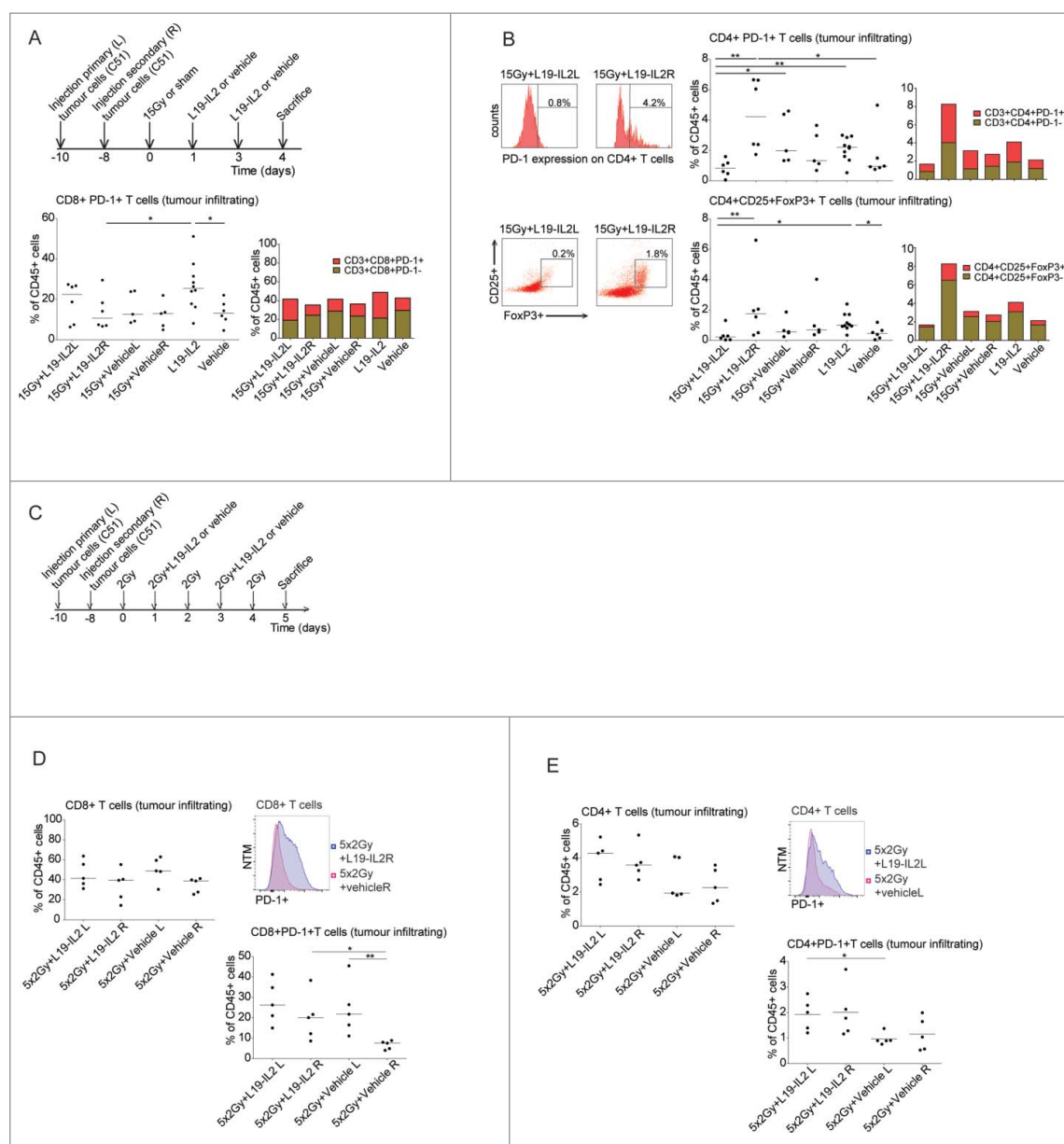


Figure 3. Co-expression of immune suppressive receptors on T cells. (A) Treatment schedule for the evaluation of immunological parameters in single dose irradiation experiments, percentage of intratumoural CD8⁺PD-1⁺ cells of the CD45⁺ cells and median percentages of PD-1⁺ and PD-1⁻ within the CD8⁺ T cell population. (B) Representative FACS histogram and dotplot, percentage of intratumoural CD4⁺PD-1⁺ cells and CD4⁺CD25⁺FoxP3⁺ T cells of CD45⁺ cells in different treatment groups and median percentages of PD-1⁺ and PD-1⁻ or CD25⁺FoxP3⁺ and CD25⁻FoxP3⁻ within the CD4⁺ T cell population. (C) Treatment schedule for the evaluation of immunological parameters in fractionated irradiation experiments. (D) Quantification of CD8⁺ T cells of gated CD45⁺ tumour infiltrating cells, FACS histogram of PD-1 expression on tumour infiltrating CD8⁺ T cells and quantification of CD8⁺PD-1⁺ cells. (E) Quantification of CD4⁺ T cells of gated CD45⁺ tumour infiltrating cells, FACS histogram of PD-1 expression on tumour infiltrating CD4⁺ T cells and quantification of CD4⁺PD-1⁺ cells. NTM: Normalized to Mode. **p*<0.05, ***p*<0.01. Bars represent median.

groups were combined. High dose RT resulted in severe skin toxicity, resulting in a 50% drop-out before tumour re-challenging. Although high dose RT resulted in not significantly different tumour take as compared with 10Gy + L19-IL2 (*p* = 0.27), low number of animals in the former group limits the interpretation of these results (Fig. 5D). In contrast, surgery + L19-IL2 induced less protective effect (i.e. greater tumour reuptake) as compared with 10Gy + L19-IL2 (*p* = 0.051). Furthermore, non-tumour bearing mice pre-treated with 10Gy + L19-IL2 were all able to form tumours (500 mm³) within 13 days, similar to control mice (matrigel + shamRT + vehicle), proving that treatment alone is not sufficient to induce memory effect without prior tumour cure (Fig. 5D).

Endpoint immunological analyses (gating strategy in supplementary Fig. 6B) revealed that higher number of peripheral (blood) CD8⁺ T cells expressed CD44⁺CD127⁺ when mice were able to reject tumours (14.6% [5.4–29.1]) after 10Gy + L19-IL2 as compared with other treatment groups (1.6% [0.6–4.2], *p* < 0.05 of all other groups) (Fig. 5E). These high co-expression levels were not found on the CD8⁺ T cells of the two mice with tumour growth after re-challenge (2.1 and 0.8%), showing that the co-expression of both receptors on CD8⁺ T cells can distinguish long-lasting immunological protection against tumours (Fig. 5E). 10Gy + L19-IL2 cured mice able to reject tumours also showed a significantly higher percentage of CD44⁺CD127⁺ on CD8⁺ T cells in spleens (48.8% [35.4–68.6]) as compared with other

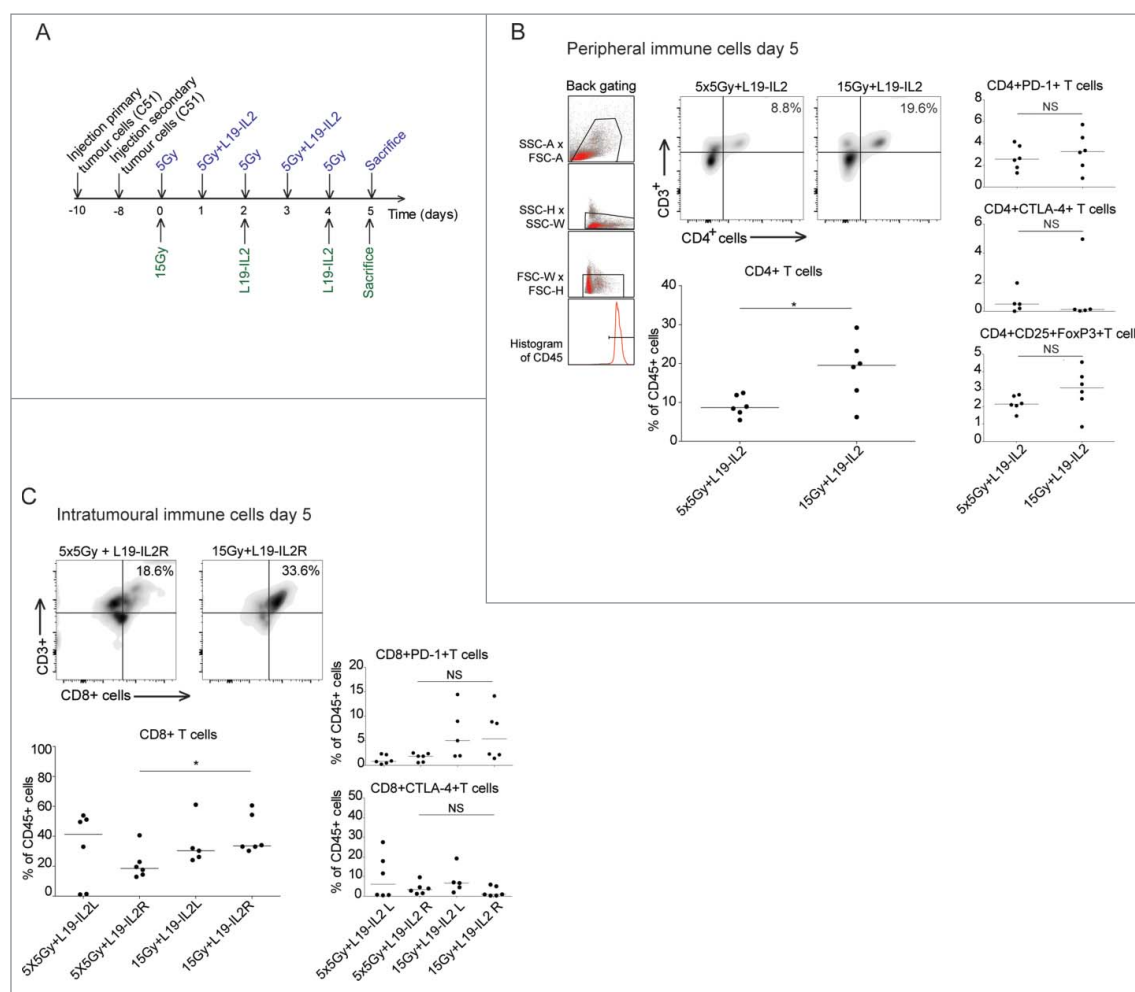


Figure 4. Immunological responses after single doses and fractionated irradiation. (A) Experimental setup and schedule for immunological analysis of tumours and blood. Representation and quantification of percentages of CD4⁺, CD4⁺ PD-1⁺, CD4⁺ CTLA-4⁺ and CD4⁺ FoxP3⁺ CD25⁺ T cells of total peripheral (B) and tumour infiltrating (C) CD45⁺ immune cells. **p* < 0.05. Bars represent median.

treatment groups (8.4% [4.6–38.5], *p* < 0.05). Again, this high co-expression level was not found on the CD8⁺ T cells of the two mice with tumour growth after re-challenge (4.5% and 5.9%) (supplementary Fig. 7). Mice cured from C51 tumours by L19 + IL2 receiving IgG instead of CD127 blockage had a significantly higher percent of CD8⁺ T co-expressing CD44⁺CD127⁺ in lymph nodes (36.7% [26.9–52.5], *p* < 0.05) as compared with all other groups except for the high dose RT upon tumour cell re-injection (supplementary Fig. 7). These results show that the CD44⁺CD127⁺ expression on CD8⁺ T cells is associated with immunological protective effect but the blockage of CD127 did not abrogate this effect.

Cytokine production and cytotoxic activity of both CD8⁺ and CD8⁺CD44⁺CD127⁺ T cells was evaluated to investigate the role of these T cells in immunological memory. For this, single cell suspensions of immune cells isolated from lymph nodes of responders (mice cured by 10Gy+L19-IL2 remaining tumour-free after re-challenge), non-responders (mice cured by 10Gy+L19-IL2 with tumour take after re-challenge) or naive mice were co-cultured with C51 cells. To test specificity of the reactions, immune cells from responders were co-cultured with 4T1 mammary carcinoma cells as an example of unspecific antigens. The percent of CD8⁺ T cells was

significantly higher when C51 cells were co-cultured with responder immune cells as compared with non-responder (*p* < 0.05) and naive (*p* < 0.05) mice, reaching marginal significance (*p* = 0.053) when compared with co-culture with unspecific antigens (Fig. 6A). These results suggest higher proliferation activity of CD8⁺ T cells from mice with specific immunological memory. As expected, a significantly (*p* < 0.01) higher percent of CD8⁺ T cells from responder mice co-expressed CD44 and CD127 (Fig. 6B). Importantly, responders showed specific and significantly (*p* = 0.006) higher percent of CD8⁺ and CD8⁺CD44⁺CD127⁺ T cells producing the cytokines INF γ , TNF α as well as the cytolytic molecule Granzyme B (Fig. 6C, D). In addition, significantly (*p* = 0.009) higher percent of CD8⁺CD44⁺CD127⁺ T cells expressing CD107a, a marker of cytotoxic activity, was found in responders co-cultured with C51 cells as compared with unspecific 4T1 cells (Fig. 6D). Altogether, these data confirm antigen-specific cytokine production and cytotoxic activity of CD8⁺CD44⁺CD127⁺ T cells from mice cured by 10Gy+L19-IL2 with memory capacity.

Significantly higher percent of CD8⁺ T cells co-expressing CD44⁺CD62 L⁺ was found in lymph nodes of cured mice able to reject tumours (7.3% [5.7–9.8] anti-CD127 group and 12.9% [6.9–21.6] IgG group) as compared with all other treatment

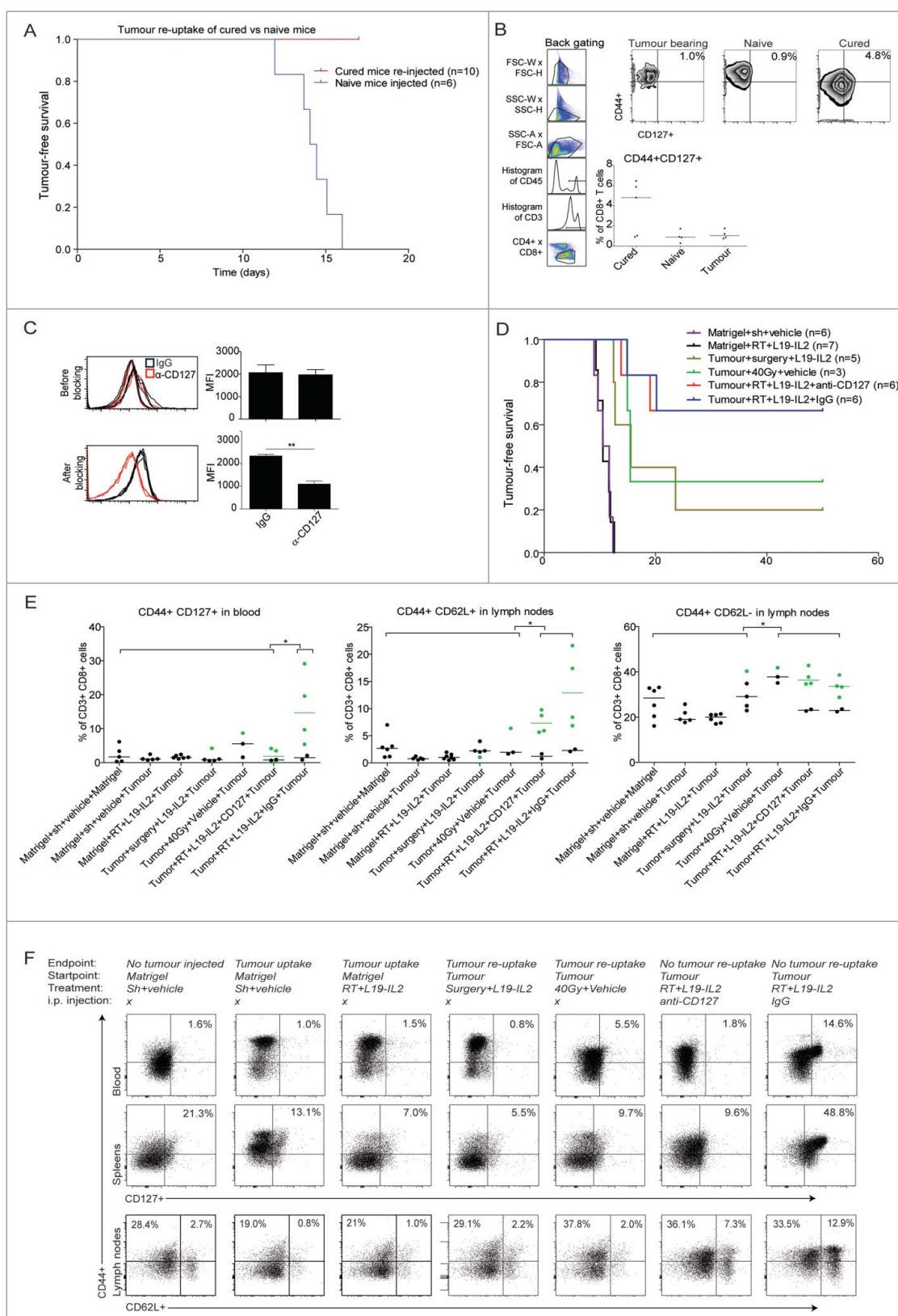


Figure 5. RT + L19-IL2 triggers long-lasting immunological memory. (A) Tumour-free survival of mice that rejected tumours after 10Gy + L19-IL2 and were re-injected at day 150 with C51 tumour cells, together with a group of naïve mice. (B) Percentage of CD44⁺CD127⁺ cells of splenic CD8⁺ T cells. (C) Confirmation of CD127 inhibition by FACS in peripheral blood at day 3 after CD127 blocking. (D) Tumour-free survival of mice that were cured after different treatments and were re-challenged at day 150 with C51 tumour cells, together with a group of control mice initially injected with matrigel only. (E) Percentages of CD44⁺CD127⁺, CD44⁺CD62L⁺ and CD44⁺CD62L⁻ of total CD8⁺ T cells in blood and lymph nodes. Green symbols represent responders (no tumour take after re-injection) and black symbols represent non-responders. Bars represent median. (F) Representative plots and median percentages of different immune subsets analyzed by FACS in blood, spleens and lymph nodes.

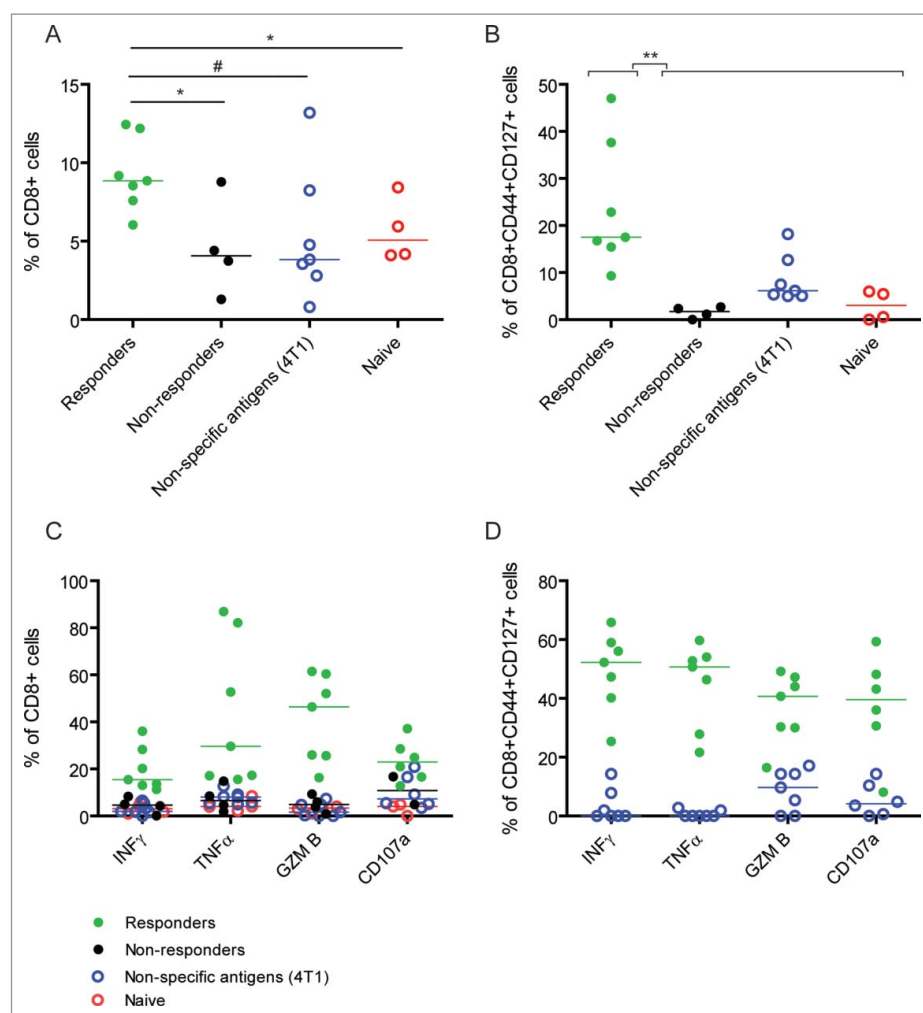


Figure 6. Specific cytokine production and cytotoxic activity of CD8⁺ and CD8⁺CD44⁺CD127⁺ T cells from mice with immunological memory. (A) Percent of CD8⁺ and (B) CD8⁺CD44⁺CD127⁺ T cells after co-culture of C51 or 4T1 (unspecific antigens) tumor cells with immune cells from responders (mice cured by 10Gy+L19-IL2 with tumor rejection after re-challenge), non-responders (mice cured by 10Gy+L19-IL2 with tumor uptake after re-challenge) and naive mice. (C) Percent of INF- γ , TNF- α , Granzyme B- (GZM B) and CD107a-positive CD8⁺ T cells after co-culture of C51 or 4T1 tumor cells with immune cells from responders, non-responders and naive mice. (D) Percent of INF- γ , TNF- α , Granzyme B- (GZM B) and CD107a-positive CD8⁺CD44⁺CD127⁺ T cells after co-culture of C51 or 4T1 tumor cells with immune cells from responders. ** $p < 0.01$, * $p < 0.05$, # $0.05 < p < 0.1$. Bars represent median.

groups (2% [1–4], $p = 0.01$). Additionally, lymph nodes contained a higher percentage of CD44⁺CD62 L⁻ T cells (36.3%, [34.5–42.8] CD127 group and 33.5% [28.7–38.6] IgG group) as compared with all other treatment groups (28.4% [17.7–40.3] (Fig. 5E, F). It appears that percentages of splenic CD44⁺CD62 L⁺ and CD44⁺CD62 L⁻ CD8⁺ T cells were higher in cured mice able to reject tumours as compared with mice with tumour take (supplementary Fig. 7). No significant differences between CD44⁺CD62 L⁺ expressing CD8⁺ T cells in blood could be observed between treatment groups (data not shown).

Discussion

Over the last years, the improved understanding of radiation-induced effects on the tumour microenvironment has resulted in the recognition that RT has a novel role as an inducer of the immunogenic death of tumour cells.⁴⁰ Since this form of cell death is capable of converting the patient's tumour into an 'in situ' vaccine, it can initiate an anti-tumour immune response,⁴¹

which may be further increased when combined with immunotherapeutic approaches.⁴⁰ The selective delivery of IL2 to tumour vascular components via the L19-IL2 fusion protein is a novel promising immunotherapy approach^{24,33,42} and can enhance the therapeutic potential of RT in ED-B positive tumours in a CD8⁺ T cell⁴³ or NK cell mediated manner.⁴⁴ These highly synergistic preclinical findings resulted in the initiation of a phase I clinical study in our institute (NCT02086721), which is currently ongoing. Since the therapeutic effect of this combination treatment is immune mediated, we hypothesized that it can elicit an abscopal effect targeting macroscopic tumours directly and preventing new tumour formation (recurrence) later on.

To test the hypotheses in the present proof-of-principle study we have used the well-established and –characterized C51 tumour model. To mimic metastasizing cancer, we implanted secondary tumours resembling metastasis (or a secondary tumour in mismatched experiments) outside the radiation field. The choice of this experimental model is governed by the possibility to control experimental conditions such as tumour volume at start of treatment and to enable precise

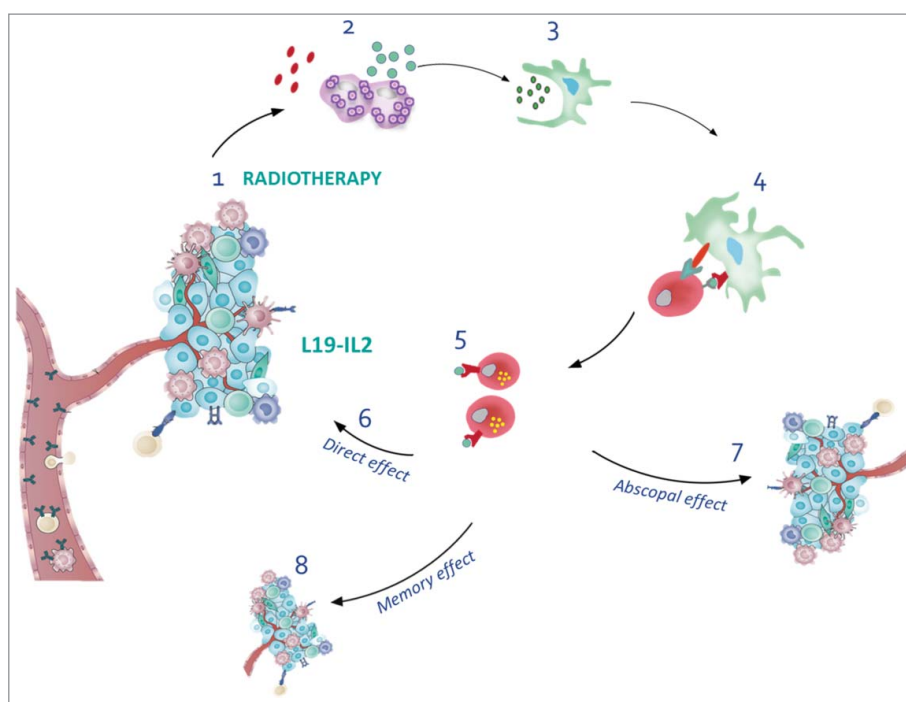


Figure 7. Overview of radiotherapy and L19-IL2 induced anti-tumour effects. (1) Radiotherapy induces immunogenic cell death, thereby releasing DAMPs and antigens (2), creating an *in situ* vaccine. Tumour-associated antigens are picked up by dendritic cells (3) that migrate to lymph nodes to activate CD8⁺ T cells (4). L19-IL2 can stimulate the proliferation of tumour specific CD8⁺ T cells (5) that can now target the irradiated tumours (6), non-irradiated tumours (7) and prevent the formation of new tumours months after tumour cure and termination of the treatment (8). Modified from.^{71, 72}

irradiation of the primary tumour as well as accurate daily tumour monitoring. Importantly, all secondary tumours were clearly macroscopic and growing, which reduces potential bias resulting from incomplete tumour take due to technical reasons.

We have investigated three different RT schedules in combination with L19-IL2 including single dose and fractionated irradiation regimens. We have shown that the single RT dose + L19-IL2 retarded significantly tumour growth outside the irradiation field and even cured 20–30% of the non-irradiated tumours. Since it is known that the RT dose, schedule and technique may provoke diverse systemic immune responses,⁵ we additionally used two fractionated RT regimes (5 × 2Gy and 5 × 5Gy) in combination with L19-IL2. Indeed, several preclinical studies showed significant growth delay and complete remission outside the RT field when immunotherapy (anti-CTLA-4) was combined with fractionated RT but not with a large single dose.^{45,46} In the present study, we have shown that a significant growth delay of tumours outside the RT field could be observed using fractionated combination treatment schedules, however, none of these tumours could be cured, suggesting that a single high radiation dose is a more potent trigger for immune-mediated curative abscopal effects. Additionally, fractionated irradiation might kill tumour infiltrating T cells, resulting in a decreased abscopal effect when combined with L19-IL2. In agreement with our results, a single RT dose (20Gy) initiated immune responses and tumour (including non-irradiated metastases) growth delay when combined with a CD8⁺ T cell activating immunotherapy.⁴⁷ This systemic anti-tumour effect was not observed when combined with fractionated RT (4 × 5Gy).⁴⁸ Differences in tumour immunogenicity, composition of immune

infiltrating cells at start of (RT) treatment,⁴⁹ RT doses and different immunotherapeutic approaches may all explain the contradictory results to induce anti-tumour effects outside the RT field between different research groups.

Mice treated with 15Gy + L19-IL2 revealed an increase in CD4⁺ but not in CD8⁺ T cell infiltration in tumours outside the RT field on day 4 after start of treatment, suggesting an association of the CD4⁺ T cells with the observed long-lasting abscopal effect. Despite we did not observe an increased percentage of CD8⁺ T cells inside the non-irradiated tumours at this time point, depletion of CD8⁺ T cells (starting at day 5) abrogated the abscopal effect of the combination therapy significantly. Furthermore, we have shown that depletion of CD4⁺ or CD8⁺ T cells at day 5 has no or little effect on tumour cure of the primary tumour. This suggests that the anti-tumour immune response against the irradiated tumour was complete at start of depletion, enabling us to follow up growth delay effects of the non-irradiated secondary tumours. These data provide direct evidence that the growth delay and complete remission of 20–30% of the non-irradiated tumours is predominantly attributed to CD8⁺ T cells and at least in part to CD4⁺ T cells.

Using the ED-B positive CT26 colon carcinoma³³ as a secondary tumour, we observed a similar growth delay of the mismatched tumour when administrating 15Gy to the primary C51 tumour in combination with L19-IL2 compared to a C51 secondary tumour. The common expression of antigen(s) between the irradiated tumour and other tumour sites may be crucial for an anti-tumour immune response outside the RT field.⁵⁰ Therefore, it is expected that the irradiated C51 tumour and the non-irradiated CT26 tumour indeed share common

tumour specific antigens which might explain similar abscopal effect observed in both experimental settings. It might be possible that secondary tumours from other origin share less antigens and respond less to abscopal response raised towards the irradiated C51 colon carcinoma, but remains to be investigated further.

In this study, we have established the importance of T cells in the execution of the specific RT + L19-IL2 mediated abscopal effect (Fig. 7). Additionally, we observed that part of these infiltrating T cells have a regulatory (FoxP3⁺CD25⁺) phenotype or they express PD-1, which is known to be associated with their exhaustion.⁵¹ PD-1 expressing T cells as well as increased infiltrate of regulatory T cells was not observed inside irradiated primary tumours, suggesting that large single radiation dose can shift the effector/regulatory balance into an effective immune response. Indeed, it is known that radiotherapy has a broad range of immune stimulating effects on the tumour microenvironment, transforming it into an immunogenic hub⁵ making it a highly attractive approach to improve immunotherapeutic efficacy, especially for less immunogenic solid tumours. However, using fractionated (5 × 2Gy) radiotherapy, we could, next to an increase of PD-1 expressing T cells inside non-irradiated tumours, additionally show an increase of PD-1 expressing T cells inside irradiated tumours. The expression of PD-1 on T cells is identified as an important resistant mechanism to radiotherapy triggered systemic anti-tumour immune responses.⁵²⁻⁵⁴ Furthermore, several PD-1 inhibitors, including nivolumab, have recently obtained FDA approval⁵⁵ and show very promising anti-tumour activity in several clinical trials.^{56,57} Therefore, a trimodal treatment using RT and L19-IL2 combined with nivolumab might be a promising approach to further increase the abscopal effect for patients with metastases. Furthermore, direct comparison between non-irradiated tumours of 15Gy and 5 × 5Gy + L19-IL2 treated mice revealed that the single RT dose treated mice have a higher percentage of peripheral CD4⁺ T cells and a higher percentage of CD8⁺ T cells infiltrating their non-irradiated tumour. Since it is well known that CD8⁺ T cells have anti-tumour activity against primary tumours,⁴³ and since we have shown in the depletion study that T cells are crucial for RT + L19-IL2 abscopal effect, these differences may explain why single RT dose leads to 20–30% cure of tumours outside the irradiation field.

Moreover, in a pilot study, we have shown that mice cured after 10Gy RT + L19-IL2 are able to develop a long-lasting immunological memory, associated with an increase in CD127 (IL-7 receptor α) expression on T cells (Fig. 5). IL7 is known to have an important role in the generation and maintenance of memory T cells as CD127 deficient mice or CD127 blockade in combination with anti-PD-1 and anti-CTLA4 bimodal treatment abolished or attenuated the ability to reject bladder tumours.⁵⁸ Non-tumour bearing mice treated with 10Gy + L19-IL2 did not develop this protective immunity, showing the importance of the tumour to form the basis for this ‘in situ’ vaccine that can eventually be translated into a direct (irradiated), indirect (non-irradiated) and long-lasting (re-challenged) anti-tumour immune response. Since we wanted to reproduce our findings of this pilot experiment, we kept this schedule (and RT dose, i.e. 10Gy) similar in our new experimental setup, however we believe that conclusion of our study would not change if mice cured after 15Gy + L19-IL2 therapy would have been re-challenged. Here, we

additionally show that RT might be a better treatment modality to trigger the initiation of the long-lasting anti-tumour immune response, since surgery + L19-IL2 showed a reduced number of mice able to reject tumour cells upon re-injection 150 days post injection. The role of surgery in the development of a memory or abscopal immune response warrants further investigations since a recent study has demonstrated that the targeted delivery of immunotherapy (anti-PD-1) to the surgically removed tumour site can induce an ‘in situ’ vaccination reducing cancer recurrence and metastases in mice.⁵⁹

Immunological analysis revealed a significantly higher percentage of CD8⁺ T cells expressing CD44⁺CD62 L⁺ and CD44⁺CD62 L⁻ in the lymph nodes of cured mice able to reject tumours after 10Gy + L19-IL2. It has been reported that effector cells have high expression of CD44 and low expression of CD62 L while central memory cells have high expression of both CD44 and CD62 L.⁶⁰⁻⁶² Therefore, it suggests that effector T cells and central memory T cells are more abundant in the lymph node compartment when mice are able to reject tumours after they are cured. Furthermore, we show that mice able to reject tumours have significantly higher percent of CD8⁺CD44⁺CD127⁺ T cells in spleens, lymph nodes and blood. It has been shown that the expression of CD44 and CD127 on CD8⁺ T cells can classify these cells as effector memory T cells,⁶⁰⁻⁶² and indeed the expression of CD127 is a hallmark of primed CD8⁺ T cells to develop into long-lived memory cells.^{60,63-65} The expression of CD44⁺CD127⁺ on CD8⁺ T cells seems to be even more pronounced in blood, making this expression profile of great interest as a potential biomarker when investigating tumour reactive memory T cells. However, blocking of CD127 of RT + L19-IL2 cured mice shortly before and after re-injection of tumours to assess involvement of the IL-7 pathway on memory T cells, could not abrogate the memory effect in the present study, i.e. increase tumour take after re-challenge. Despite of this, we confirmed the antigen-specific cytokine production and cytotoxic activity of CD8⁺CD44⁺CD127⁺ T cells, suggesting their involvement in immunological memory.

To conclude, this study shows for the first time that irradiation results in a curative abscopal effect when combined with systemic L19-IL2 treatment dependent on T cells in 20–30% of the mice. Single dose RT combined with L19-IL2 leads to an elevation of T cell infiltration in the non-irradiated tumours with a more immunosuppressive phenotype, a phenomenon which is enhanced upon fractionated irradiation. We suggest that diminished abscopal effect in fractionated irradiation is likely due to fractionation than to the total radiation dose since the total dose, biologically equivalent to the large single dose, has been applied. Finally, in this study we have shown that RT + L19-IL2 can induce a long-lasting immunological protection against tumours, which is associated with the presence of effector and central memory T cells.

Materials and methods

Tumour cell lines/ reagents/ Antibodies for in vivo studies

Exponentially growing C51 and CT26 mouse colon carcinoma cell lines (kindly provided by Philogen S.p.A.) syngeneic to the Balb/c mice were cultured in Dulbecco's

Modified Eagle Medium (DMEM) and Roswell Park Memorial Institute (RPMI) (Lonza), respectively, supplemented with 10% fetal calf serum (FCS) in a humidified 5% CO₂ chamber at 37°C.

The L19-IL2 immunocytokine (Philogen S.p.A.) was diluted with sterile phosphate buffered saline (PBS, Lonza) to concentrations of 200 µg/ml. For *in vivo* depletion experiments, the monoclonal antibodies anti-CD8a (clone YTS 169.4), anti-CD4 (clone YTS 191) and the isotype control anti-KLH rat IgG2b (clone LTF-2) (BioXCell) were diluted with sterile PBS to a concentration of 1.67 mg/ml. For *in vivo* blocking experiments, the monoclonal anti-CD127 (clone A7R34) and rat IgG2a isotype control (clone 2A3) antibodies (BioXCell) were diluted with sterile PBS to a concentration of 2 mg/ml. All studies were conducted in a laboratory that operates under exploratory research principles using established laboratory protocols and general research investigative assays.

Mice and in vivo experiments

All experiments were performed in accordance with local institutional guidelines for animal welfare and were approved by the Animal Ethical Committee of the University of Maastricht, the Netherlands, and were in accordance with the Helsinki Declaration of 1975 as revised in 2000. In all *in vivo* experiments tumour growth was monitored daily. Tumour size was measured using a Vernier caliper until endpoint, defined as time to reach 4 times starting volume (T4xSV). Tumour volume was calculated using the following formula: $(\pi/6) \times \text{length} \times \text{width} \times \text{height}$, each dimension corrected for the skin thickness (0.5 mm). Animals with cured tumours were excluded from the growth delay analysis, but were included as ‘censored’ animals in the Kaplan-Meier survival analysis. All irradiations were performed using Varian Truebeam linear accelerator (15 MeV) electrons and the tumour volumes at start of irradiation are summarized in supplementary table 1.

Determination of 100% curative RT dose for primary tumors

To induce tumours, approximately 8 weeks old immunocompetent female Balb/c mice (Harlan Laboratories) were subcutaneously (s.c.) injected with C51 cells (1.5×10^6) suspended in Basement Membrane Matrix (Matrigel™, BD Biosciences) 10 days prior to RT (day -10) bilaterally. For all these growth delay experiments, tumour volumes were normalized to day of irradiation (day 0). Tumours were irradiated with a single dose of 15Gy on day 0 or 5 × 2Gy (one fraction per day) fractionated RT, combined with systemic therapy L19-IL2 (20 µg per mouse intravenously (i.v.) as previously tested³³) or vehicle (PBS) on day 1, 3 and 5. For these studies 5 mice (bilateral tumors, 10 tumours in total) per RT schedule were investigated.

Abscopal effect study

Syngeneic C51 cells (1.5×10^6) were injected as described above 10 days prior to RT in the left flank (primary tumour). Two days later right flank was injected s.c. with C51 cells (1.5×10^6) (secondary abscopal tumour). This design has been chosen to obtain secondary tumours of smaller sizes at time of irradiation to mimic metastases in cancer patients and used by others combining radiotherapy with immunotherapy to study abscopal effect.⁶⁶⁻⁶⁸ Only

the left tumours of the mice were irradiated. Mice were treated with 15Gy + L19-IL2 (n = 10), 15Gy + vehicle (n = 9), 5 × 2Gy + L19-IL2 (n = 8), 5 × 2Gy + vehicle (n = 10). To be able to compare tumour responses between 15Gy single dose and a fractionated regime we calculated dose per fraction to be delivered once a day for 5 days that results in the same biological effect as single dose RT using the linear quadratic formalism.⁶⁹ We assumed that the α/β ratio of mouse tumours equals to 10Gy. Dose recovered per day due to proliferation (D_{prolif}) was not taken into account in calculations because published data on repopulation of mouse tumours demonstrated that repopulation rate in differentiated adenocarcinomas, mammary carcinoma and in fast fibrosarcoma did not increase in the first week of radiotherapy.⁷⁰ This fractionated schedule (5 × 5Gy) was added in an additional experiment and delivered only to the left tumour in combination with L19-IL2 (n = 6).

To evaluate the causal relationship between CD4⁺ or CD8⁺ T cells and tumour growth delay of the non-irradiated secondary tumours, anti-CD4 (0.2 mg per mouse, intraperitoneal [i.p.]) and anti-CD8 (0.2 mg per mouse, i.p.) antibodies were injected on days 5, 8 and 11. Depletion of the cells was confirmed by flow cytometry analysis (see below) of blood collected via puncture of the saphenous vein. Tumour volume data were normalized to start of depletion (day 5). In total 20 mice were used in the depletion study, 6–7 mice per group.

The results of the abscopal study have been validated in 2 independent experiments (vide supra).

To investigate the specificity of the abscopal response, C51 cells (1.5×10^6) were injected s.c. on day -10 in the left flank (irradiated tumour) and syngeneic CT26 cells (2×10^6) were injected s.c. on day -8 in the right flank (non-irradiated tumour) of the mice. Mice were treated with 15Gy + vehicle (n = 5) or 15Gy + L19-IL2 (n = 8).

Memory effect study

For the immune memory effect study, animals were challenged in the left flank with matrigel or PBS only or with C51 tumour cells (1.5×10^6) suspended in matrigel. When tumours reached an average volume of 200 mm³, different treatment schedules were delivered as depicted in supplementary Fig. 6. Long-term surviving animals after treatment with surgery (see below) + L19-IL2 (n = 5), high dose RT (40Gy) + vehicle (n = 3) and 10Gy + L19-IL2 (n = 12) were re-challenged bilaterally with C51 cells (1.5×10^6) 150 days post injection in their left and right flanks. The latter group was divided in two, one group receiving CD127 blocking antibody (0.4 mg, i.p.) (n = 6) and the other receiving rat IgG2a isotype control (n = 6) one day before tumour re-challenge and then every 2 days for 3 weeks. Blockade of CD127 was confirmed in CD3⁺ peripheral blood mononuclear cells in blood extracted by saphenous vein puncture after second dose of blocking antibody had been delivered. In addition, age-matched non-tumour bearing mice (only matrigel injected) treated with 10Gy RT + L19-IL2 (n = 7) or sham + vehicle (n = 6) were included as control groups. Tumour growth was monitored as described above. In survival analysis, tumor take was considered as an event when tumor reached 500 mm³. All animals not reaching this endpoint were free of tumor. Only the fastest growing tumour of the two bilaterally (re-)injected tumours was used for analyses. The results

of the memory study have been validated in 2 independent experiments (vide supra).

Surgical excision of tumours

Before surgical excision of tumours, the skin around the tumour was shaved and the area was disinfected with 70% ethanol. All surgical procedures were done under general anesthesia with isoflurane inhalation. The surgical area was sterilized with iodine solution and a sterilized scalpel was used to make an elliptic incision around the tumour to dissect it away from the flank. To stop the bleeding, an electrocautery was used to close blood vessels and the surgical incision was closed by stitching using the U-stich with an absorbable suture. Post-operative care of the animals included the administration of 300 mg/kg paracetamol.

Flow cytometry

Flow cytometric analysis was performed on immune cells isolated from spleens, lymph nodes, blood and tumours. First, animals treated with 15Gy + L19-IL2 (n = 6), 15Gy + vehicle (n = 5), L19-IL2 (n = 3) and vehicle (n = 5) were sacrificed on day 4. Second, animals treated with 5 × 2Gy + vehicle (n = 5) and 5 × 2Gy + L19-IL2 (n = 5) treatment groups were sacrificed on day 5. A third flow cytometry experiment was performed comparing 15Gy + L19-IL2 (n = 6) with 5 × 5Gy + L19-IL2 (n = 6) on day 5.

Blood was collected in 10% Heparin sodium (5000 I.U./ml, Leo Laboratories Ltd.) and plasma was separated by centrifugation. Single cell suspensions of lymph nodes, spleens and tumours were obtained using a gentleMACS dissociator (Miltenyi Biotec B.V.) and filtered through a 70 µm-pore cell strainer (Greiner, Bio-one). Additionally, tumours were enzymatically digested with a tumour dissociation kit (Miltenyi Biotec B.V.) before making single cell suspensions. Red blood cells lysis was performed on single cell suspensions of blood, spleens and tumours using RBC lysis buffer (eBioscience). Single cell suspensions were counted using a Z2 Coulter Counter (Beckman). $1.5\text{--}2 \times 10^6$ cells were stained with PBS containing 2% FCS, incubated with FC-block CD16/CD32 (clone 2.4G2, BD Biosciences) and stained with a combination of the following antibodies for cell surface markers: anti-CD45-V500, PE, FITC, APC and PE-Cy7 (clone 30F-11), anti-CD3-FITC (17A2), anti-CD4-APC-H7 (GK1.5), anti-CD8a-V500 (53-6.7), anti-CD19-PE (1D3), anti-CD25-APC (PC61), anti-CD44 APC-Cy7 (IM7), anti-CD127-PE (clone SB/199) and anti-CD127-PE (A7R34) (BD Biosciences); anti-NKp46-APC (29A1.4.9, Miltenyi Biotec B.V.); anti-CD45-PerCP (30-F11), anti-CD152 (CTLA-4)-Brilliant Violet 421 (UC10-4B9) and anti-279 (PD-1)-PE-Cy7 (RMP1-30) (Biolegend); anti-CD3e- eFLUO 450 (145-2c11), anti-CD4-FITC (RM4-5), anti-CD62 L-PE-Cy7 (Mel-14) (eBioscience). For intracellular staining, FC blockade and cell surface markers staining was performed, cells were washed with a fixation/permeabilization working solution (eBioscience) according to manufacturer's guidelines and then stained with anti-mouse/rat FoxP3-PE staining set (FJK-16s, eBioscience). Eight-colour flow cytometric analysis was performed with a FACSCanto II instrument (BD Biosciences). Data were analyzed with

FACSDiva v6.1.2 (BD Biosciences) and FlowJo v10.0.8 (Tree Star) software. The total CD45⁺ immune cells were selected from the viable population of cells (filtered for debris and doublets) for further sub-classification according to the strategy described previously.⁴³ Staining to assess the expression of immune memory markers was performed on freshly isolated and thawed samples of spleens and lymph nodes and flow cytometric analysis yielded similar results. Gating strategies are described in Supplementary Figs. 5, 6.

Co-culture assay to assess cytokine production and cytotoxic activity of tumour specific CD8⁺ T cells

In memory study, frozen single cell suspensions of immune cells from lymph nodes of responders (long-term tumour-free survivors treated with 10Gy+L19-IL2 after re-challenge), non-responders (mice cured by 10Gy+L19-IL2 with tumour take after re-challenge) or naive mice were thawed, washed and rested overnight at 37°C in RPMI 1640 medium supplemented with 10% FCS, 1% penicillin and streptomycin, 1% L-glutamine, 50 µM of 2-mercaptoethanol and 10³ IU/ml of human recombinant IL-2 (Novartis). The next day, 10⁶ immune cells were co-cultured for 5 days in the same medium with 2.5×10^5 C51 cells (4:1 ratio) irradiated with a single dose of 50Gy. To assess non-specific antigen reactivity, a co-culture experiment of responder lymphocytes with 4T1 mammary carcinoma cells was included. After 5 days of co-culture, cells were harvested, washed and re-stimulated overnight with freshly 50Gy irradiated C51 or 4T1 cells in the presence of GolgiPlug (1 µl/ml, BD Biosciences). For FACS analysis, cells were harvested, washed with PBS and stained with LIVE/DEAD Fixable Aqua Dead Cell Stain kit (L/D Aqua, Life Technologies) according to the manufacturer's instructions, to exclude dead cells from the analysis. Cells were washed with PBS-2% FCS, incubated with Fc Block anti-CD16/32 (2.4G2, BD Bioscience) and then stained with conjugated monoclonal antibodies for cell surface markers: anti-CD8a PerCP (53-6.7), anti-CD127 PE (SB/199), anti-CD44 APC-Cy7 (IM7), anti-CD107a PE-Cy7 (1D4B) (all from BD Biosciences). Cells were then fixed and permeabilized as described above and stained for the expression of IFN-γ, TNF-α and Granzyme B, with the following monoclonal antibodies: anti-IFN-γ FITC (XMG1.2), anti-TNF-α APC (MP6-XT22) (Biolegend) and anti-Granzyme B eFluor 450 (NKZB, eBioscience). Gating strategies are described in Supplementary Fig. 8.

Statistical analysis

Statistical analyses were performed using GraphPad Prism Software v5.03. For all immune parameters and tumour volumes median [min-max] are reported. The non-parametric Mann-Whitney two-tailed test was used to determine the statistical differences between the different treatment groups. The log-rank (Mantel-Cox) test was used to compare survival curves. P-values smaller than 0.05 were considered statistically significant.

Disclosure of potential conflicts of interest

No potential conflicts of interest were disclosed.

Acknowledgments

Authors acknowledge financial support from ERC advanced grant (ERC-ADG-2015, n° 694812 – Hypoximmuno), the European Program H2020-2015-17 (ImmunoSABR – n° 733008), the European Union's Horizon 2020 research and innovation program Marie Skłodowska-Curie (Radiation Innovations for Therapy and Education, RADIATE - no. 642623) and Kankeronderzoekfonds Limburg from the Health Foundation Limburg.

Funding

EU H2020, 733008.

ORCID

Nicolle H. Rekers  <http://orcid.org/0000-0003-4172-151X>

Ludwig J. Dubois  <http://orcid.org/0000-0002-8887-4137>

References

- Demaria S, Formenti SC. Radiation as an immunological adjuvant: current evidence on dose and fractionation. *Front Oncol.* 2012;2:153. doi:10.3389/fonc.2012.00153.
- Kaur P, Asea A. Radiation-induced effects and the immune system in cancer. *Frontiers in oncology.* 2012;2:191. doi:10.3389/fonc.2012.00191.
- Krysko DV, Garg AD, Kaczmarek A, Krysko O, Agostinis P, Vandenabeele P. Immunogenic cell death and DAMPs in cancer therapy. *Nat Rev Cancer.* 2012;12:860–75. doi:10.1038/nrc3380.
- Green DR, Ferguson T, Zitvogel L, Kroemer G. Immunogenic and tolerogenic cell death. *Nat Rev Immunol.* 2009;9:353–63. doi:10.1038/nri2545.
- Demaria S, Golden EB, Formenti SC. Role of Local Radiation Therapy in Cancer Immunotherapy. *JAMA Oncol.* 2015;1:1325–32. doi:10.1001/jamaoncol.2015.2756.
- Chandra RA, Wilhite TJ, Balboni TA, Alexander BM, Spektor A, Ott PA, Ng AK, Hodi FS, Schoenfeld JD. A systematic evaluation of abscopal responses following radiotherapy in patients with metastatic melanoma treated with ipilimumab. *Oncoimmunology.* 2015;4:e1046028. doi:10.1080/2162402X.2015.1046028.
- Demaria M, Ohtani N, Youssef SA, Rodier F, Toussaint W, Mitchell JR, Laberge RM, Vijg J, Van Steeg H, Dollé ME, et al. An essential role for senescent cells in optimal wound healing through secretion of PDGF-AA. *Dev Cell.* 2014;31:722–33. doi:10.1016/j.devcel.2014.11.012.
- Demaria S, Ng B, Devitt ML, Babb JS, Kawashima N, Liebes L, Formenti SC. Ionizing radiation inhibition of distant untreated tumors (abscopal effect) is immune mediated. *Int J Radiat Oncol Biol Phys.* 2004;58:862–70. doi:10.1016/j.ijrobp.2003.09.012.
- Mole RH. Whole body irradiation; radiobiology or medicine? *Br J Radiol.* 1953;26:234–41. doi:10.1259/0007-1285-26-305-234.
- Okuma K, Yamashita H, Niibe Y, Hayakawa K, Nakagawa K. Abscopal effect of radiation on lung metastases of hepatocellular carcinoma: a case report. *J Med Case Rep.* 2011;5:111. doi:10.1186/1752-1947-5-111.
- Wersall PJ, Blomgren H, Pisa P, Lax I, Kalkner KM, Svedman C. Regression of non-irradiated metastases after extracranial stereotactic radiotherapy in metastatic renal cell carcinoma. *Acta Oncol.* 2006;45:493–7. doi:10.1080/02841860600604611.
- Grass GD, Krishna N, Kim S. The immune mechanisms of abscopal effect in radiation therapy. *Curr Probl Cancer.* 2016;40:10–24. doi:10.1016/j.crrp.2015.10.003.
- Ehlers G, Fridman M. Abscopal effect of radiation in papillary adenocarcinoma. *Br J Radiol.* 1973;46:220–2. doi:10.1259/0007-1285-46-543-220.
- Kingsley DP. An interesting case of possible abscopal effect in malignant melanoma. *Br J Radiol.* 1975;48:863–6. doi:10.1259/0007-1285-48-574-863.
- Nobler MP. The abscopal effect in malignant lymphoma and its relationship to lymphocyte circulation. *Radiology.* 1969;93:410–2. doi:10.1148/93.2.410.
- Ohba K, Omagari K, Nakamura T, Ikuno N, Saeki S, Matsuo I, Kinoshita H, Masuda J, Hazama H, Sakamoto I, et al. Abscopal regression of hepatocellular carcinoma after radiotherapy for bone metastasis. *Gut.* 1998;43:575–7. doi:10.1136/gut.43.4.575.
- Rees GJ. Abscopal regression in lymphoma: a mechanism in common with total body irradiation? *Clin Radiol.* 1981;32:475–80. doi:10.1016/S0009-9260(81)80310-8.
- Sham RL. The abscopal effect and chronic lymphocytic leukemia. *Am J Med.* 1995;98:307–8. doi:10.1016/S0002-9343(99)80380-5.
- Vatner RE, Cooper BT, Vanpouille-Box C, Demaria S, Formenti SC. Combinations of immunotherapy and radiation in cancer therapy. *Front Oncol.* 2014;4:325. doi:10.3389/fonc.2014.00325.
- Carnemolla B, Borsi L, Balza E, Castellani P, Meazza R, Berndt A, Ferrini S, Kosmehl H, Neri D, Zardi L, et al. Enhancement of the antitumor properties of interleukin-2 by its targeted delivery to the tumor blood vessel extracellular matrix. *Blood.* 2002;99:1659–65. doi:10.1182/blood.V99.5.1659.
- Rosenberg SA. IL-2: the first effective immunotherapy for human cancer. *J Immunol.* 2014;192:5451–8. doi:10.4049/jimmunol.1490019.
- Weber JS, Yang JC, Topalian SL, Schwartzentruber DJ, White DE, Rosenberg SA. The use of interleukin-2 and lymphokine-activated killer cells for the treatment of patients with non-Hodgkin's lymphoma. *J Clin Oncol: official journal of the American Society of Clinical Oncology.* 1992;10:33–40. doi:10.1200/JCO.1992.10.1.33.
- Alwan LM, Grossmann K, Sageser D, Van Atta J, Agarwal N, Gilreath JA. Comparison of acute toxicity and mortality after two different dosing regimens of high-dose interleukin-2 for patients with metastatic melanoma. *Target Oncol.* 2014;9:63–71. doi:10.1007/s11523-013-0276-7.
- Johannsen M, Spitaleri G, Curigliano G, Roigas J, Weikert S, Kempkensteffen C, Roemer A, Kloeters C, Rogalla P, Pecher G, et al. The tumour-targeting human L19-IL2 immunocytokine: preclinical safety studies, phase I clinical trial in patients with solid tumours and expansion into patients with advanced renal cell carcinoma. *Eur J Cancer.* 2010;46:2926–35. doi:10.1016/j.ejca.2010.07.033.
- Borsi L, Balza E, Bestagno M, Castellani P, Carnemolla B, Biro A, Lepri A, Sepulveda J, Burrone O, Neri D, et al. Selective targeting of tumoral vasculature: comparison of different formats of an antibody (L19) to the ED-B domain of fibronectin. *Int J Cancer.* 2002;102:75–85. doi:10.1002/ijc.10662.
- Danielli R, Patuzzo R, Ruffini PA, Maurichi A, Giovannoni L, Elia G, Neri D, Santinami M. Armed antibodies for cancer treatment: a promising tool in a changing era. *Cancer Immunol, Immunother: CII.* 2015;64:113–21. doi:10.1007/s00262-014-1621-0.
- Eigentler TK, Weide B, de Braud F, Spitaleri G, Romanini A, Pflugfelder A, González-Iglesias R, Tasciotti A, Giovannoni L, Schwager K, et al. A dose-escalation and signal-generating study of the immunocytokine L19-IL2 in combination with dacarbazine for the therapy of patients with metastatic melanoma. *Clin Cancer Res.* 2011;17:7732–42. doi:10.1158/1078-0432.CCR-11-1203.
- Weide B, Eigentler TK, Pflugfelder A, Zelba H, Martens A, Pawelec G, Giovannoni L, Ruffini PA, Elia G, Neri D, et al. Intralesional treatment of stage III metastatic melanoma patients with L19-IL2 results in sustained clinical and systemic immunologic responses. *Cancer Immunol Res.* 2014;2:668–78. doi:10.1158/2326-6066.CIR-13-0206.
- Danielli R, Patuzzo R, Di Giacomo AM, Gallino G, Maurichi A, Di Florio A, Cutaia O, Lazzeri A, Fazio C, Miracco C, et al. Intralesional administration of L19-IL2/L19-TNF in stage III or stage IVM1a melanoma patients: results of a phase II study. *Cancer Immunol, Immunother: CII.* 2015;64:999–1009. doi:10.1007/s00262-015-1704-6.
- Bentzen AK, Marquard AM, Lyngaa R, Saini SK, Ramskov S, Donia M, Such L, Furness AJ, McGranahan N, Rosenthal R, et al. Large-scale detection of antigen-specific T cells using peptide-MHC-I multimers labeled with DNA barcodes. *Nat Biotechnol.* 2016;34:1037–45. doi:10.1038/nbt.3662.
- Robbins PF, Lu YC, El-Gamil M, Li YF, Gross C, Gartner J, Lin JC, Teer JK, Cliften P, Tycksen E, et al. Mining exomic sequencing data to identify mutated antigens recognized by adoptively transferred tumor-reactive T cells. *Nat Med.* 2013;19:747–52. doi:10.1038/nm.3161.
- Vogelstein B, Papadopoulos N, Velculescu VE, Zhou S, Diaz LA, Jr., Kinzler KW. Cancer genome landscapes. *Science.* 2013;339:1546–58. doi:10.1126/science.1235122.

33. Zegers CM, Rekers NH, Quaden DH, Lieuwes NG, Yaromina A, Germeraad WT, Wieten L, Biessen EA, Boon L, Neri D, et al. Radiotherapy combined with the immunocytokine L19-IL2 provides long-lasting antitumor effects. *Clin Cancer Res.* 2015;21:1151–60. doi:10.1158/1078-0432.CCR-14-2676.
34. Santimaria M, Moscatelli G, Viale GL, Giovannoni L, Neri G, Viti F, Leprini A, Borsi L, Castellani P, Zardi L, et al. Immunoscintigraphic detection of the ED-B domain of fibronectin, a marker of angiogenesis, in patients with cancer. *Clin Cancer Res: an official journal of the American Association for Cancer Research.* 2003;9:571–9.
35. Rossin R, Berndorff D, Friebe M, Dinkelborg LM, Welch MJ. Small-animal PET of tumor angiogenesis using a (76)Br-labeled human recombinant antibody fragment to the ED-B domain of fibronectin. *J Nucl Med: official publication, Society of Nuclear Medicine.* 2007;48:1172–9. doi:10.2967/jnumed.107.040477.
36. Pujuguet P, Hammann A, Moutet M, Samuel JL, Martin F, Martin M. Expression of fibronectin ED-A+ and ED-B+ isoforms by human and experimental colorectal cancer. Contribution of cancer cells and tumor-associated myofibroblasts. *Am J Pathol.* 1996;148:579–92.
37. Johnson EE, Yamane BH, Buhtoiarov IN, Lum HD, Rakhmilevich AL, Mahvi DM, Gillies SD, Sondel PM. Radiofrequency ablation combined with KS-IL2 immunocytokine (EMD 273066) results in an enhanced antitumor effect against murine colon adenocarcinoma. *Clin Cancer Res: an official journal of the American Association for Cancer Research.* 2009;15:4875–84. doi:10.1158/1078-0432.CCR-09-0110.
38. El-Emir E, Dearling JL, Huhlov A, Robson MP, Boxer G, Neri D, van Dongen GA, Trachsel E, Begent RH, Pedley RB. Characterisation and radioimmunotherapy of L19-SIP, an anti-angiogenic antibody against the extra domain B of fibronectin, in colorectal tumour models. *Brit J Cancer.* 2007;96:1862–70. doi:10.1038/sj.bjc.6603806.
39. Schwager K, Hemmerle T, Aebischer D, Neri D. The Immunocytokine L19-IL2 Eradicates Cancer When Used in Combination with CTLA-4 Blockade or with L19-TNF. *J Invest Dermatol.* 2013;133:751–8. doi:10.1038/jid.2012.376.
40. Formenti SC, Demaria S. Combining Radiotherapy and Cancer Immunotherapy: A Paradigm Shift. *J Natl Cancer Inst.* 2013. doi:10.1093/jnci/djs629.
41. Formenti SC, Demaria S. Systemic effects of local radiotherapy. *Lancet Oncol.* 2009;10:718–26. doi:10.1016/S1470-2045(09)70082-8.
42. Eigentler TK, Weide B, de Braud F, Spitaleri G, Romanini A, Pflugfelder A, González-Iglesias R, Tasciotti A, Giovannoni L, Schwager K, et al. A dose-escalation and signal-generating study of the immunocytokine L19-IL2 in combination with dacarbazine for the therapy of patients with metastatic melanoma. *Clin Cancer Res.* 2011;17:7732–42. doi:10.1158/1078-0432.CCR-11-1203.
43. Zegers CM, Rekers NH, Quaden DH, Lieuwes NG, Yaromina A, Germeraad WT, Wieten L, Biessen EA, Boon L, Neri D, et al. Radiotherapy combined with the immunocytokine L19-IL2 provides long-lasting antitumor effects. *Clin Cancer Res.* 2015;21:1151–60. doi:10.1158/1078-0432.CCR-14-2676.
44. Rekers NH, Zegers CM, Yaromina A, Lieuwes NG, Biemans R, Senden-Gijsbers BL, Losen M, Van Limbergen EJ, Germeraad WT, Neri D, et al. Combination of radiotherapy with the immunocytokine L19-IL2: Additive effect in a NK cell dependent tumour model. *Radiother Oncol: journal of the European Society for Therapeutic Radiology and Oncology.* 2015;116(3):438–42. doi:10.1016/j.radonc.2015.06.019.
45. Demaria S, Kawashima N, Yang AM, Devitt ML, Babb JS, Allison JP, Formenti SC. Immune-mediated inhibition of metastases after treatment with local radiation and CTLA-4 blockade in a mouse model of breast cancer. *Clin Cancer Res.* 2005;11:728–34.
46. Mencacci A, Montagnoli C, Bacci A, Cenci E, Pitzurra L, Spreca A, Kopf M, Sharpe AH, Romani L. CD80+Gr-1+ myeloid cells inhibit development of antifungal Th1 immunity in mice with candidiasis. *J Immunol.* 2002;169:3180–90. doi:10.4049/jimmunol.169.6.3180.
47. Yu P, Lee Y, Wang Y, Liu X, Auh S, Gajewski TF, Schreiber H, You Z, Kaynor C, Wang X, et al. Targeting the primary tumor to generate CTL for the effective eradication of spontaneous metastases. *J Immunol.* 2007;179:1960–8. doi:10.4049/jimmunol.179.3.1960.
48. Lee Y, Auh SL, Wang Y, Burnette B, Meng Y, Beckett M, Sharma R, Chin R, Tu T, Weichselbaum RR, et al. Therapeutic effects of ablative radiation on local tumor require CD8+ T cells: changing strategies for cancer treatment. *Blood.* 2009;114:589–95. doi:10.1182/blood-2009-02-206870.
49. Schae D, Ratikan JA, Iwamoto KS, McBride WH. Maximizing tumor immunity with fractionated radiation. *Int J Radiat Oncol, Biol, Phys.* 2012;83:1306–10. doi:10.1016/j.ijrobp.2011.09.049.
50. Demaria S, Formenti SC. Can abscopal effects of local radiotherapy be predicted by modeling T cell trafficking? *J Immunother Cancer.* 2016;4:29. doi:10.1186/s40425-016-0133-1.
51. Picarda E, Ohaegbulam KC, Zang X. Molecular Pathways: Targeting B7-H3 (CD276) for Human Cancer Immunotherapy. *Clin Cancer Res: an official journal of the American Association for Cancer Research.* 2016;22(14):3425–31. doi:10.1158/1078-0432.CCR-15-2428.
52. Dovedi SJ, Adlard AL, Lipowska-Bhalla G, McKenna C, Jones S, Cheadle EJ, Stratford IJ, Poon E, Morrow M, Stewart R, et al. Acquired resistance to fractionated radiotherapy can be overcome by concurrent PD-L1 blockade. *Cancer Res.* 2014;74:5458–68. doi:10.1158/0008-5472.CAN-14-1258.
53. Park SS, Dong H, Liu X, Harrington SM, Krco CJ, Grams MP, Mansfield AS, Furutani KM, Olivier KR, Kwon ED. PD-1 Restrains Radiotherapy-Induced Abscopal Effect. *Cancer Immunol Res.* 2015;3:610–9. doi:10.1158/2326-6066.CIR-14-0138.
54. Taube JM, Anders RA, Young GD, Xu H, Sharma R, McMiller TL, Chen S, Klein AP, Pardoll DM, Topalian SL, et al. Colocalization of inflammatory response with B7-h1 expression in human melanocytic lesions supports an adaptive resistance mechanism of immune escape. *Sci Transl Med.* 2012;4:127ra37. doi:10.1126/scitranslmed.3003689.
55. Sharma P, Allison JP. The future of immune checkpoint therapy. *Science.* 2015;348:56–61. doi:10.1126/science.aaa8172.
56. Borghaei H, Paz-Ares L, Horn L, Spigel DR, Steins M, Ready NE, Chow LQ, Vokes EE, Felip E, Holgado E, et al. Nivolumab versus Docetaxel in Advanced Nonsquamous Non-Small-Cell Lung Cancer. *N Engl J Med.* 2015;373:1627–39. doi:10.1056/NEJMoa1507643.
57. Motzer RJ, Escudier B, McDermott DF, George S, Hammers HJ, Srinivas S, Tykodi SS, Sosman JA, Procopio G, Plimack ER, et al. Nivolumab versus Everolimus in Advanced Renal-Cell Carcinoma. *N Engl J Med.* 2015;373:1803–13. doi:10.1056/NEJMoa1510665.
58. Shi LZ, Fu T, Guan B, Chen J, Blando JM, Allison JP, Xiong L, Subudhi SK, Gao J, Sharma P. Interdependent IL-7 and IFN-gamma signalling in T-cell controls tumour eradication by combined alpha-CTLA-4+alpha-PD-1 therapy. *Nat Commun.* 2016;7:12335. doi:10.1038/ncomms12335.
59. Wang C, Sun W, Ye Y, Hu Q, Bomba HN, Gu Z. In situ activation of platelets with checkpoint inhibitors for post-surgical cancer immunotherapy. 2017;1:0011.
60. Kaech SM, Tan JT, Wherry EJ, Konieczny BT, Surh CD, Ahmed R. Selective expression of the interleukin 7 receptor identifies effector CD8T cells that give rise to long-lived memory cells. *Nat Immunol.* 2003;4:1191–8. doi:10.1038/ni1009.
61. Sallusto F, Lenig D, Forster R, Lipp M, Lanzavecchia A. Two subsets of memory T lymphocytes with distinct homing potentials and effector functions. *Nature.* 1999;401:708–12. doi:10.1038/44385.
62. Wherry EJ, Teichgraber V, Becker TC, Masopust D, Kaech SM, Antia R, von Andrian UH, Ahmed R. Lineage relationship and protective immunity of memory CD8T cell subsets. *Nat Immunol.* 2003;4:225–34. doi:10.1038/ni889.
63. Huster KM, Busch V, Schiemann M, Linkemann K, Kerksiek KM, Wagner H, Busch DH. Selective expression of IL-7 receptor on memory T cells identifies early CD40L-dependent generation of distinct CD8+ memory T cell subsets. *Proc Natl Acad Sci U S A.* 2004;101:5610–5. doi:10.1073/pnas.0308054101.
64. Lang KS, Recher M, Navarini AA, Harris NL, Lohning M, Junt T, Probst HC, Hengartner H, Zinkernagel RM. Inverse correlation between IL-7 receptor expression and CD8T cell exhaustion during persistent antigen stimulation. *Eur J Immunol.* 2005;35:738–45. doi:10.1002/eji.200425828.
65. Madakamutil LT, Christen U, Lena CJ, Wang-Zhu Y, Attinger A, Sundarajan M, Ellmeier W, von Herrath MG, Jensen P, Littman

- DR, et al. CD8alpha-mediated survival and differentiation of CD8 memory T cell precursors. *Science*. 2004;304:590–3. doi:10.1126/science.1092316.
66. Dovedi SJ, Cheadle EJ, Popple A, Poon E, Morrow M, Stewart R, et al. Fractionated radiation therapy stimulates anti-tumor immunity mediated by both resident and infiltrating polyclonal T-cell populations when combined with PD1 blockade. *Clin Cancer Res*. 2017. doi:10.1158/1078-0432.CCR-16-1673.
67. Twyman-Saint-Victor C, Rech AJ, Maity A, Rengan R, Pauken KE, Stelekati E, Benci JL, Xu B, Dada H, Odorizzi PM, et al. Radiation and dual checkpoint blockade activate non-redundant immune mechanisms in cancer. *Nature*. 2015;520:373–7. doi:10.1038/nature14292.
68. Vanpouille-Box C, Alard A, Aryankalayil MJ, Sarfraz Y, Diamond JM, Schneider RJ, Inghirami G, Coleman CN, Formenti SC, Demaria S. DNA exonuclease Trex1 regulates radiotherapy-induced tumour immunogenicity. *Nature Commun*. 2017;8:15618. doi:10.1038/ncomms15618.
69. Joiner CM VdKA. Fractionation: the linear-quadratic approach. *Basic clinical radiobiology* 4th ed Boca Raton: CRC Press; pp 102–119. 2009.
70. Trott KR, Kummermehr J. Rapid repopulation in radiotherapy: a debate on mechanism. Accelerated repopulation in tumours and normal tissues. *Radiother Oncol: journal of the European Society for Therapeutic Radiology and Oncology*. 1991;22:159–60.
71. Barker HE, Paget JT, Khan AA, Harrington KJ. The tumour microenvironment after radiotherapy: mechanisms of resistance and recurrence. *Nat Rev Cancer*. 2015;15:409–25. doi:10.1038/nrc3958.
72. Larson SM, Carrasquillo JA, Cheung NK, Press OW. Radioimmunotherapy of human tumours. *Nat Rev Cancer*. 2015;15:347–60. doi:10.1038/nrc3925.